Molecular Simulations of Hydrocarbon-Water Interface

A thesis submitted towards partial fulfilment of
BS-MS Dual Degree Programme

by

Mohit Dixit

under the guidance of

Dr. Kunj Tandon

Shell Technology Centre, Bangalore

Indian Institute of Science Education and Research
Pune

Certificate

This is to certify that this thesis entitled "Molecular Simulations of Hydrocarbon-Water Interface"submitted towards the partial fulfilment of the BS-MS dual degree programme at the Indian Institute of Science Education and Research Pune represents original research carried out by "Mohit Dixit" at "Shell Technology Centre, Bangalore", under the supervision of "Dr. Kunj Tandon" during the academic year 2013-2014.

Student
Mohit Dixit

Supervisor
Dr. Kunj
Tandon

Acknowledgements

Foremost, I would like to express my sincere gratitude to my advisor Dr. Kunj Tandon for the continuous support for my thesis, study and research, for his patience, motivation, enthusiasm, and immense knowledge. His guidance helped me in all the time of research and writing of this thesis. I could not have imagined having a better advisor and mentor for my 5th year M.S. project.

Besides my advisor, I would like to thank the rest of my cEOR team at Shell: Dr. Foram Thakkar, Dr. Nitish Nair and Dr. Majeed Shaik, for their encouragement, insightful comments, and hard questions.

My sincere thanks also goes to Dr. Vetrivel Rajappan, and Dr. Vianney Koelman, for offering me the internship opportunity in their group and leading me working on this exciting project.

I thank our collaboraters at Culgi B.V.: Dr. Ruben Serral Gracia and Dr. Janwillem Handgraaf, for their support with the simulation packages. I would also like to thank Dr. Sundaram Balasubramanian, Karthik Kumar and Rajdeep Payal at JNCASR, Bangalore, and Dr. Apratim Chatterji at IISER-Pune, for our fruitful discussion on the project.

Completing this work would have been all the more diffcult were it not for the support and friendship provided by the all the members of the Computational Centre of Expertise(CCOE) team. I am indebted to them for their help.

Abstract

Oil recovery, especially in the case of Secondary and Tertiary oil receovery operations, is dependent on the interaction of oil with brine or other injection fluids. The properties of the interface formed from crude oil and the brine strongly affect the economic feasibility of the oil recovery. Interfacial tension (IFT) measurement is the traditional way to quantify the interaction between oils and brine.

In hydrocarbon industry, we use estimates of IFT between oil and brine in many situations. Currently resistivity logs are the best estimates for hydrocarbon content in reservoirs. In cases where resistivity logs are not feasible, saturation height function measurements yield an estimate of the hydrocarbon content. Analysis of saturation height function measurements requires IFT values between oil and brine under reservoir conditions.

Crude oils consist of a physical mixture of a large number of chemical species. The IFT between crude oil and brine is dominated by surface active components from the mixture. Thus, it is important to understand the interaction of various components of crude oils at the brine-hydrocarbon interface.

Reliable estimates of IFT between hydrocarbon and brine are critical to many such workflows in hydrocarbon industry. Considering the importance of obtaining accurate estimates of IFT between oil and brine in reservoir conditions, we recently started a concerted effort to derive predictive methods for IFT. The objective of this program is to demonstrate the feasibility of accurate IFT predictions, starting with atomistic models for oils and brine. In the first phase of this program we worked with simple oils, namely n-alkanes as, to validate methods, forcefields and models. We have developed a multi-scale predictive modeling protocol to predict IFT and density of hydrocarbons. We have demonstrated the accuracy of the methods to be within 2% of experimental values and IFT predictions to within 10% of experimental values. The accuracy of density and IFT predictions are maintained even for elevated temperatures and pressures, prevalent in hydrocarbon reservoirs.

After we had validated the protocols and models, we used the predictive methods to study the effect of molecules from alkyl phenol family. A variety of alkyl phenols are known to be prevalent in crude oils. By structural characteristics, these species turn out to be surface active at the interface of brine and oil. We have used our atomistic methods to study the effect of various topological factors on the surface activity of alkyl phenols. We have used, IFT as a measure of surface activity in these cases.

In future, these developed methods can be applied to Oil-Brine system instead of Oil-Water systems. We can observe the effects of the salinity on the interfacial behavior by including reliable models for dissociated salt species .These methods can also be used to study the relative interactions between various surface active species existing in crude-oils.

Contents

Chapter 1

Introduction

Many industrial processes depend on detailed understanding of interfacial properties for interfaces of immiscible liquids. Oil-in-water emulsions are extremely important in food industry. Both, oil-in-water as well as water-in-oil emulsions, are found in energy industry. The nature of emulsion, which depends on the conditions of the physical mixtures, has implications on the viability of commercial operations. As an example, economic recovery of crude oil from oil reservoirs is dependent on the interactions of crude oil, water, the rock and other chemical species present at the interfaces[1]. Thus understanding the fundamental interactions dominating emulsions of crude oil and saline water, is the first step to developing economically sustainable energy options for future.

There has been a lot of scientific research in the field of ultra-low IFT[2][3] [4]. For the present discussion, ultralow IFT is 10^{-2} - 10^{-3} dynes/cm. Ultra-low IFTs result from an optimal mixture of surfactants at oil-water interface in most of the cases. In such cases the emulsions are commonly referred to as microemulsions. Typical interfacial tensions for n-alkanes and water are in the order of about 50 dynes/cm. In case of microemulsions however, this IFT reduces by about 4 orders of magnitude to 10^{-3} dynes/cm. The compositional range of mixtures, over which such microemulsions form, is usually very limited. Hence it is critical to develop methods for understanding of the effect of important components on the interfacial properties. Crude oils contain a wide range of chemicals, and hence the methods used in this endeavor span computational as well as experimental domains.

Conventional experimental methods for measuring IFT are in the domain of drop shape analysis to infer the IFT between interfaces. There are broadly two categories of methods 1. pendant drop for the interfaces with IFT above 10^{-2} dynes/cm and, 2. spinning drop method for IFTs below 10^{-2} dynes/cm. These methods are time consuming. Also considering the vast number of components in typical crude oils, it is difficult to analyze the effect of individual species. By applying computational methods, we are able to study inter-facial properties of crude oil $\&$ water systems efficiently and in ways that are easy to scale over multiple formulations. Also computational methods are easy to deploy in cases where specific oil components are not easy to isolate.

Some of the species in crude oils are considered more surface active than others. These partition onto the interface in a ratio higher than their bulk concentrations. Some examples of such chemical species are (a)Phenols, (b)Carbazoles, (c)Naphthenic acids and, (d)Asphaltenes. These could be considered natural sur-

factants existing in the crude oils. These are special classes of molecules which are both hydrophobic and hydrophilic known as surfactants. IFT plays an important role in determining the oil recovery in from reservoirs. IFT is probably the most important measure of interaction of brine with crude oils. Low IFT is usually desirable for oil recovery. This is especially true in case of water flooding used for enhanced oil recovery(EOR).

In this study, we start by demonstrating the accuracy of atomistic computational methods, in predicting IFTs at different temperature and pressure conditions. We have used Hexane, Nonane and Dodecane as model oil in our study. We have validated a protocol which integrates Coarse-grained method like Dissipative Particle Dynamics(DPD) with Molecular Dynamics(MD). While Coarse Grained technique like DPD will be time-efficient and will equilibrate the system faster, MD will be accurate in terms of system behavior and property calculation. This is known as multi-scale modeling. We have also screened down OPLS-AA as suitable Force Field(FF) for in molecular simulations for predicting IFTs.

We evaluated the accuracy of these methods by comparing with experimental values of physical properties reported in literature. The density predictions from MD simulations were within 2 $\%$ of experimental value and IFT predictions to within 10 $\%$ of experimental values.

We then applied computational methods to study the effect of molecules from nonyl-phenol family on the IFT. These molecules belong to non-ionic class of surfactants. They have hydrophilic hydroxyl group as well as hydrophobic alkyl chain. Hence, they arrange themselves at the interface in order to reduce the interfacial tension of the system.

Here, we have studied the effect of the addition of 3 isomers of Nonyl-Phenol which are (a) para-linear Nonyl-Phenol, (b) para-branched Nonyl-Phenol and, (c) ortho-linear Nonyl-Phenol. We have chosen these isomers so that we can study the effect of topology of surfactants on the Oil-Water interface. We have investigated the interfacial behavior of oil-water system by adding these species and calculating interfacial tension of these systems. We have also compared the surface efficiency of these surfactants for Nonane-Water systems which is defined as the reduction in the IFT value for a particular concentration of alkyl-phenol in bulk oil.

In this report, we have briefly discussed elements of DPD and MD methods in "theory" section. The "computational methods" section provides details of simulation and discussions on the optimization of parameters in MD. In the last section, we demonstrate the validity the protocol and force field by comparing with experimental IFT values where available. We also demonstrate the effect of Phenol and Nonyl-Phenol on the Oil-Water interface. We conclude that ortho-linear and para-branched Nonyl-Phenol are more surface efficient in reducing IFT than para-linear Nonyl-Phenol.

Chapter 2

Computational Methods

This section discusses the computational methods incorporated to study interfacial properties of Oil-Water systems. We provide details of the multi-scale modeling which we have have incorporated in our protocol. DPD and MD techniques are discussed in separate sections. We also discuss the optimization of input parameters in both methods to arrive at reliable physical propeties. As test case for the validity of the input parameters, we have used simple-oils namely n-alkanes at the interface of water. In this case reliable experimental data is available for density and IFT for a number of alkanes.

2.1 Multi-scale modeling

Molecular Dynamics(MD) and Monte Carlo(MC) are two main methods which are being used investigate the statistical mechanics of complex condensed phase and biochemical systems[5]. A great amount of modern research in material sceince is based on the results of these methods or extend these methods to larger systems or larger run-time.

Schematic Fig. 2.1 below shows various length and time scale accessible in computational simulations[6]. The choice of simulation method is based on specific probelm at hand, as well as the computational resources at disposal.

As seen in the Fig. 2.1, electronic structure calculations cover the shortest length and time scales. These calculations are deployed in cases where the exchange of electrons is key to the underlying science. As example would be the situation of modeling catalysts.

In the present situation our aim is to accurately calculate bulk physical properties like IFT, density. Thus MD simulations are the tool of choice. As we study systems with large number of molecules or systems with large molecules, MD becomes computationally demanding. In such cases, Coarse Grained(CG) methods like DPD and Brownian Dynamics (BD) are typically deployed.

One can, in principle, also merge two of these techniques to calculate properties taking advantage of both techniques. While CG technique will be time-efficient and will equilibrate the system faster, MD will be accurate in terms of system behavior and property calculation. This is known as multi-scale modeling.

Anticipating the complexity of oils that are of interest in RDS, we have chosen to develop a hybrid protocol of DPD and MD simulations. DPD is deployed initially

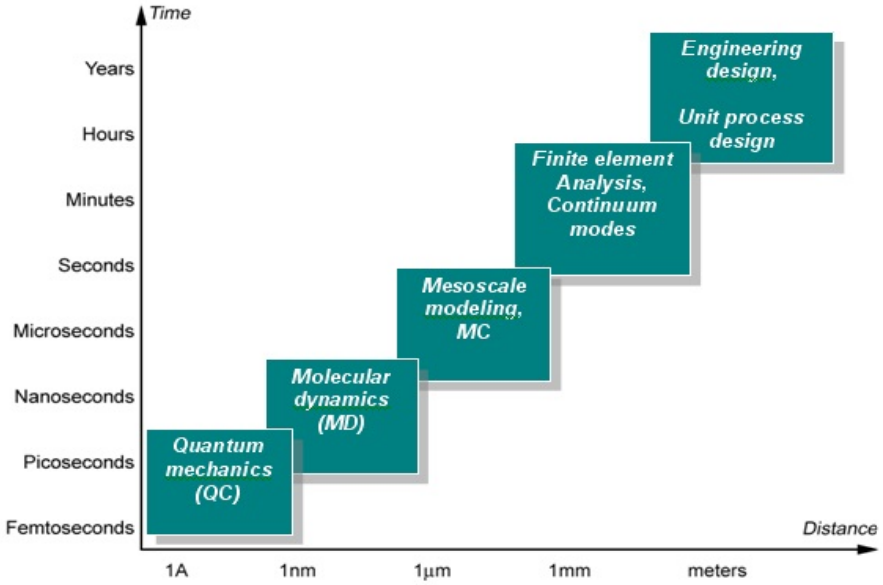

Figure 2.1: **Length-scales with time-scales in Molecular Mechanics(MM) showing various methods. It goes on from QC calculations to Engineering design. We have used used MD and MC for our purposes.**

to obtain equilibrium configurations of systems rapidly. We map the equilibrated DPD simulation box to an atomistic simulation box for the MD simulations for predicting physical properties. The overall multi-scale protocol has significant savings in compute time since the equilibration is not accomplished at the highest level of accuracy.

2.2 Dissipative Particle Dynamics(DPD)

Dissipative Particle Dynamics(DPD) is a particle-based mesoscopic simulation technique which was developed by Hoogerbrugge and Koelman to study properties of complex fluids efficiently in Shell[7]. Each DPD bead represents group of atoms or molecules. The coarse graining of the structures allowed the bigger systems to be simulated for longer time than is possible with Molecular Dynamics(MD). Interactions between the beads are soft and represented through a repulsion term. This repulsion has a linear form. This is different from the forcefields in MD, discussed later.

In DPD, the dynamics of the DPD system is controlled by Newton's equation of motions[8]:

$$\frac{\delta r_i}{\delta t} = v_i, m_i \frac{\delta v_i}{\delta t} = f_i \tag{2.1}$$

Where r_i, m_i and v_i are position, mass and velocity corresponding to bead i, respectively. The force acting on bead i is f_i which is the summation of three pairwise forces i.e. conservative force F^C, dissipative force F^D and random force F^R.

$$f_i = \sum_{i \neq j} (F_{ij}^C + F_{ij}^D + F_{ij}^R) \tag{2.2}$$

This sum runs over all neighboring particles within interaction range r_C. The conservative force, F_k^c is usually soft repulsive of the form

$$F_k^c = \begin{cases} \alpha_{ij}(1 - r_{ij}/r_c)\hat{r_{ij}} & : r_{ij} < r_c \\ 0 & : r_{ij} > r_c \end{cases}$$

Where α_{ij} is the maximum repulsion term between beads i and j. r_{ij} would be the distance between them and r_c is the cut-off radius which shows the extent of interaction range. The dissipative force F^D is directly proportional to the relative velocities of the beads and tries to reduce the relative momentum. The random force F^R gives energy input to the system and acts as a thermostat with dissipative force.

$$F_{ij}^D = \gamma \omega^D(r_{ij})(\hat{r_{ij}}.\vec{v_{ij}})\hat{r_{ij}} \tag{2.3}$$

$$F_{ij}^R = \sigma \omega^R(r_{ij})\theta_{ij} \triangle t^{-1/2} \hat{r} \tag{2.4}$$

Where $v_{ij} = v_i - v_j$, σ is the noise amplitude, γ is the dissipative parameter, $\omega^D(r_{ij})$ and $\omega^R(r_{ij})$ are weighting functions which becomes zero for $r > r_c$ and θ_{ij} is the random Gaussian variable with zero mean.

In our studies, we have used three different oils for validation namely hexane, nonane and dodecane. We first start by filling the simulation box with Oil and Water beads with bead density of 3.0 beads per grid. Oil and Water beads and their mapping to the atomistic level has been shown in Fig. 2.2 and 2.3 below.

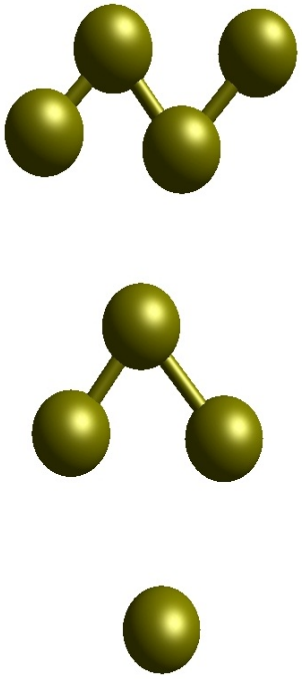

Figure 2.2: **Softcore bead representation of dodecane, nonane and water**

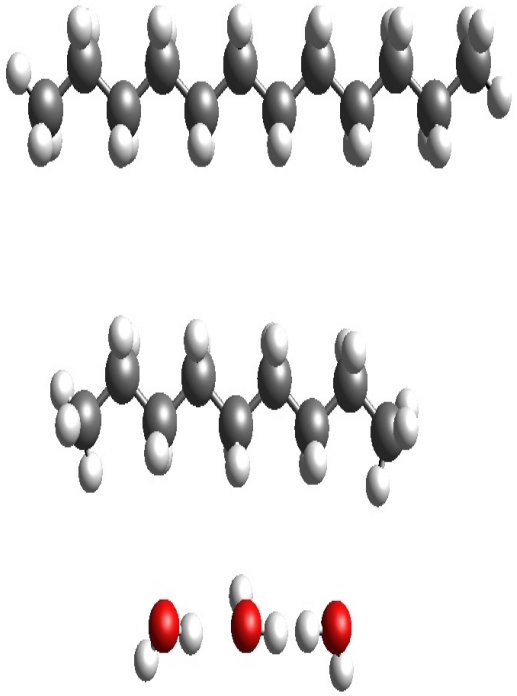

Figure 2.3: **Atomistic representation of dodecane, nonane and water**

As depicted in Fig. 2.2 and 2.3, we have chosen to assign three carbon atoms and related hydrogens to a single Soft Core(SCM) bead. So while Dodecane has 2 terminal and 2 intermediate beads, Nonane has 2 terminal and 1 intermediate beads and Hexane has only two terminal beads. Three water molecules has been assigned as one bead in our DPD simulations. The simulation box has been divided into three slabs: first one-fourth and last one-fourth is filled with water while the rest of is filled with oil.

Here, we have also explained how the Phenol softcore beads were mapped to the atomistic level. In the Fig. 2.4(a), we have first shown the softcore bead representation of the Phenol molecule. Fig. 2.4(b) and 2.4(c) shows the individual mapping of each of the two beads to the allyl and hydroxy-allyl groups which are at the atomistic level. Fig. 2.5 shows the atomistic structure of Phenol which has been obtained by connecting allyl and hydroxy-allyl group through yellow colored connectors.

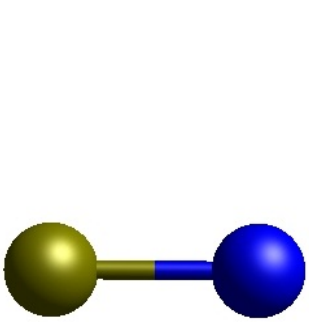

(a) Phenol softcore bead

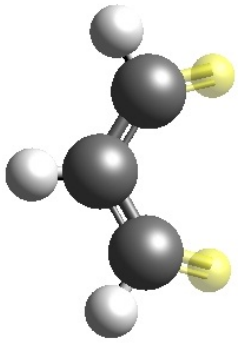

(b) allyl group

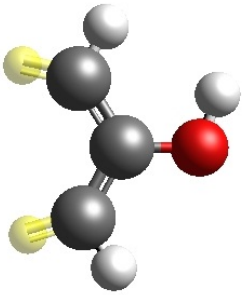

(c) hydroxyallyl group

Figure 2.4: **Softcore bead representation of (a) Phenol molecule and mapping of Phenol softcore bead to the atomistic level which results in (b) allyl and (c) hydroxy-allyl group. In (a), light green and blue colored bead are allyl and hydroxyallyl groups respectively. Grey spheres represent carbon atoms, white spheres represent hydrogen atoms and red represents oxygen.**

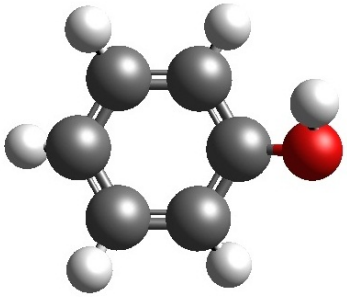

Figure 2.5: **Atomistic representation of Phenol molecule which has been obtained by combining allyl and hydroxy-allyl groups using yellow colored connectors. Grey spheres represent carbon atoms, white spheres represent hydrogen atoms and red represents oxygen.**

We have investigated Phenol-Oil-Water systems as well as Alkyl-Phenol-Oil-Water systems. We have studied 3 isomers of Nonyl-Phenol which are (a) para-linear Nonyl-Phenol molecule, (b) para-branched Nonyl-Phenol molecule and (c) ortho-linear Nonyl-Phenol molecule. The structures of these isomers are shown in Fig. 2.6, 2.7 and 2.8.

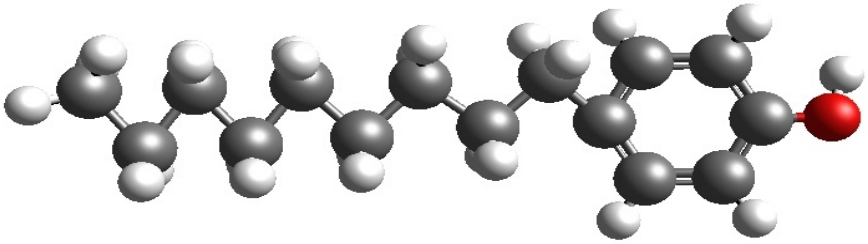

Figure 2.6: **Atomistic representation of para-linear nonyl-phenol molecule used in the simulations. Grey spheres represent carbon atoms, white spheres represent hydrogen atoms and red represents oxygen.**

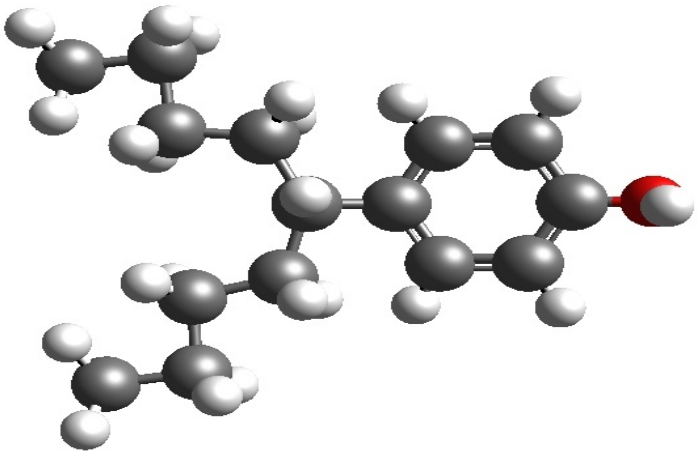

Figure 2.7: **Atomistic representation of para-branched nonyl-phenol molecule used in the simulations. Grey spheres represent carbon atoms, white spheres represent hydrogen atoms and red represents oxygen.**

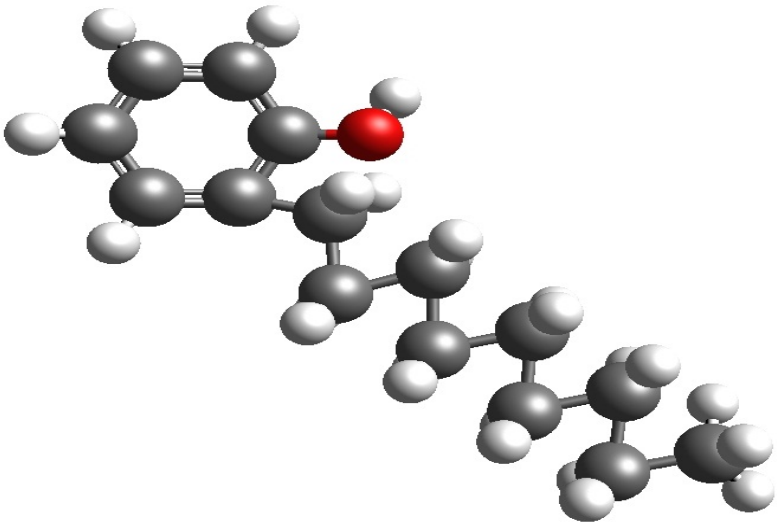

Figure 2.8: **Atomistic representation of ortho-linear nonyl-phenol molecule used in the simulations. Grey spheres represent carbon atoms, white spheres represent hydrogen atoms and red represents oxygen.**

We created the softcore beads for these molecules by attaching the alkyl chains

to the appropriate places. For example, we have created para-linear Nonyl-Phenol and para-branched Nonyl-Phenol molecules by attaching the linear and branched nonyl group to the middle carbon atom of the allyl group, respectively. Similarly, we have obtained ortho-linear Nonyl-Phenol molecules by attaching linear nonyl group to the terminal carbon atom of the hydroxy-allyl group. The simulation box during DPD simulations looks like shown in Fig. 2.9.

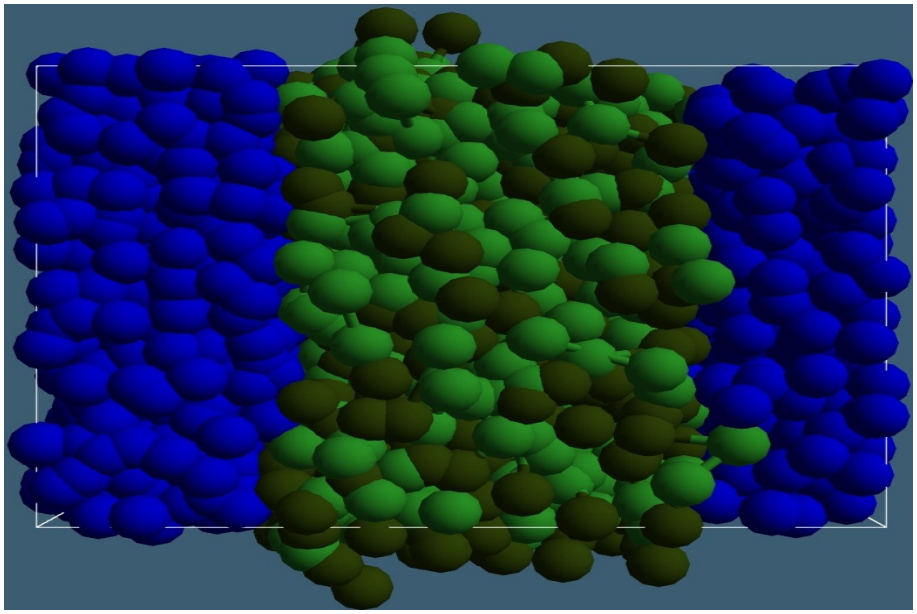

Figure 2.9: **A snapshot of Oil-Water system before DPD simulation. Green and dark green SCM(soft core molecule) beads are the carbon beads for dodecane molecule. Here, green SCM bead is "intermediate SCM bead" which consists of 3 carbon atoms which are all intermediate carbon atoms (present in the middle of the dodecane chain). The dark green SCM bead is "terminal SCM bead" which consists of 3 carbon atoms out of which one is terminal (at one of the ends of the dodecane chain). The reason for the differentiation between the intermediate and terminal SCM beads is due to the fact that the interactions of water with these two SCM beads is different and is shown with different repulsion parameters. The blue SCM bead represents 3 water molecules.**

The starting configuration of molecules in the box is such that the oil and water regions are separated. The water region is in the middle half of the box, while the oil spans the left quarter and right quarter of the box, along x-axis. This is a choice only to ease the calculation of IFT. Also the liquid interface is designed not to coincide with the box edge. These two choices help the computation while not affecting the physics.

2.3 Molecular Dynamics(MD)

MD is a microscopic modeling method in which the trajectories of atoms/molecules are studied and governed by solving equations of motion numerically [9][10][11]. MD method have been widely popular in science fraternity for mainly two reasons. These simulations provides the insight into the motions of individual particles as a function of time and hence these systems can be studied far more easily than the experiments to investigate the property of the system in detail. Secondly, although the potentials used in these simulations are approximate, the parameters (Force field(FF) parameters) can be calibrated to calculate the particular property that the user is interested in. For example, some of the FFs are good at calculating viscosity of complex fluids while some of them are good at calculating inter-facial properties.

MD simulations begin with the understanding of change in the energy of the system as a function of atomic co-ordinates. The different possible stable and metastable structures are determined by the changes in the potential energy of the system. The forces acting on the particles, which is the first derivative of the potential energy of the system, are used to see the dynamical behavior of the system by solving newton's equations of motions as a function of time.[11] The potential energy form for a multi-atom system is given by:

$$E = E_{bond} + E_{angle} + E_{non-bonded} + E_{torsion} + E_{improper} \tag{2.5}$$

Where the total potential of system is the sum of different constituent potentials mainly divided into bonded and non-bonded interactions which consists of bond, angle, non-bonded(like van der Waals and Lennard-Jones potentials), torsional and improper terms.

So In simple terms, MD involves iterative numerical calculation of the instantaneous forces in a system. Even after making substantial amount of approximations, classical MD is still very much efficient. Quantum effects are ignored. Instead each paticle is considered to be a point mass particle which is justified from Born-Oppenheimer approximation(i.e., only the nuclear displacements need to be considered). In this section, we discuss implementation of the calculation of dynamics in MD.[12]

Assuming an atom i with mass m_i and position r_i(a 3 dimensional vector), the relationship between atom's velocity and momentum p_i will be

$$\frac{dr_i}{dt} = \frac{p_i}{m_i} \tag{2.6}$$

and the net force F_i on the atom i exerted by the whole system will be negative of the first gradient of potential energy with respect to the position of the atom i

$$F_i = -\frac{dE}{dr_i} \tag{2.7}$$

The Newtonian equation of motion for atom i will be

$$\frac{dp_i}{dt} = F_i \tag{2.8}$$

One component x (which is the single component of the vector r_i) can be expanded in the form of taylor series as a function of time-step in the following manner.

$$x(t+\triangle t) = x(t) + \frac{dx(t)}{dt}\triangle t + \frac{d^2x(t)}{dt^2}\frac{\triangle t^2}{2} + ... \tag{2.9}$$

The position $x(t)$, velocity $dx(t)/dt$ and acceleration $d^2x(t)/t^2$ are enough to solve numerical solutions of equations of motions if the approximation for the higher terms in Taylor series can be made. For single direction, Newton's second law describes the acceleration as

$$\frac{d^2x(t)}{dt^2} = \frac{F_x}{m} \tag{2.10}$$

where F_x is the x-direction component of the net force acting on the atom. However it does not account for the higher terms in the Taylor series. We can truncate the series at third term(acceleration) and go on with the dynamics of the system but this not a proper estimation which leads to poor results. Several alternate methods or numerical algorithms has been devised to overcome this shortcoming. Verlet algorithm in one such method for integrating equations of motions. A simple Verlet algorithm uses atomic positions and accelerations from time t and atomic positions from previous step $x(t-\triangle t)$ to calculate the new positions at $t+\triangle t$,

$$x(t+\triangle t) = 2x(t) - x(t-\triangle t) + \frac{d^2x(t)}{dt^2}\triangle t^2 \tag{2.11}$$

A slight modification of this is leap-frog algorithm which uses the positions at time t and velocity at time $t-\triangle t/2$ to update positions and velocities through the calculated forces $F(t)$ acting on the atoms at time t.

$$x(t+\triangle t) = x(t) + \frac{dx(t)}{dt}(t+\triangle t/2)\triangle t \tag{2.12}$$

$$\frac{dx(t)}{dt}(t+\triangle t/2) = \frac{dx(t)}{dt}(t-\triangle t/2) + \frac{d^2x(t)}{dt^2}\triangle t \tag{2.13}$$

All of the above mentioned integrators are time-reversible i.e if the signs of velocity terms are to be reversed, the system can be traced back to the initial starting configurations. This is the reason for MD to be called as deterministic method unlike Monte Carlo(which is probabilistic).

Typically MD simulations scale as a O(N^2) where N is the number of particles. As MD simulations consists of large number of particles, it is very computationally inefficient to study complex systems like ours using MD alone. This is the reason, we have used DPD and MD simulations in tandem to study our systems. While the former helps in equilibrating the system much faster, the later helps in doing production runs and calculating inter-facial properties with well-established set of FF parameters.

MD simulations are done after DPD to study interfacial phenomena by mapping the DPD box to MD box i.e. we use scripts which maps beads into atoms maintaining the box size, co-ordinates etc. This box uses Periodic Boundary Conditions(PBC) in MD and half of it is filled with Oil while the rest of it is filled with Water. The simulation box after mapping looks like shown in Fig. 2.10.

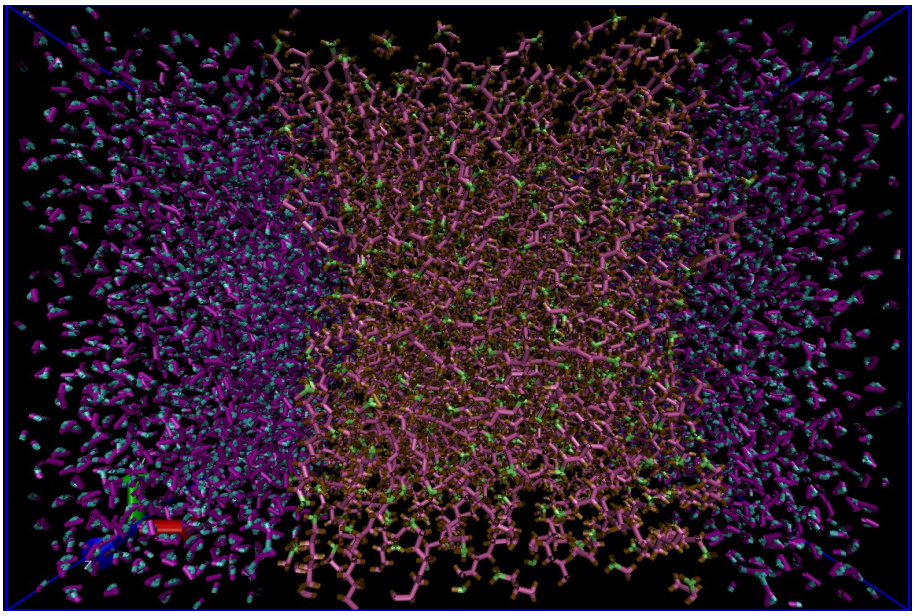

Figure 2.10: **A snapshot of Oil-Water system at the start of MD simulation. Middle region is filled with oil(dodecane) of which middle carbon atoms has been been shown in pink color while the terminal carbon atoms are in green color. The reason for the differentiation between intermediate and terminal carbons is due to the fact that these carbon atoms are treated differently in FF and are represented by different FF parameters in MD. Magenta and blue colored entities makes water molecules which are on the left and right side of the box.**

2.3.1 Force Fields

The accuracy of the potential energy function is of utmost importance to the validity of MD simulations. The form of energy function should be simple enough for computation purpose. A Force Field(FF) consists of transferable parameters for molecular sub-units, usually at the atomistic level. They are designed to be applicable to a variety of molecular systems over a range of thermodynamic conditions.Force fields usually consist of two parts; a functional form, where aspects of the molecular geometry, such as bonds, angles, torsions etc, are each assigned a mathematical function. The second aspect is a set of parameters, whose values vary depending on the atomic elements in question.

Most Force Fields(FF) used in the simulations for complex fluids share a significant number of similarities (in terms of functional form of the potential energy function). Bond and angle terms are described by harmonic term while a Fourier series describes the torsion terms. The pair-wise atomic interactions are described using Lennard-Jones function and Coulombic function. Usually, the FF parameters with the aim of predicting specific physical properties accurately e.g. OPLS-AA and CHARMM are better in capturing stress related properties of n-alkanes while TraPPE is better in determining viscosities of the same system.

The parameters of a particular FF are adjusted such that the full simulation system reproduce desired experimental observables. The direct transfer of parameters from one FF to another is, in general, not valid.

Force field selection was one key area for us and we screened several options. As we are investigating Oil-Water interface in which we also want to introduce some surfactants like phenols and sulfonates, we chose to pick correct set of FF parameters which provide us with correct interfacial and bulk properties.

We have used the all atom potential OPLS-AA force field for all of the hydrocarbon molecules and TIP3P original for modelling water molecules. In this section, we will discuss some of the FFs which are being used for Oil-Water interface in current molecular dynamics community in the world. In the end, we will reason out that why we want to go ahead with some particular FF (or more of them). This section discusses the functional forms of force fields typically used in MD simulations in materials science.

Generally the total energy of the system is calculated/expressed through two components

$$E = E_b + E_{nb} \tag{2.14}$$

Where the total energy is the sum of bonded(denoted by E_B and non-bonded E_{NB} terms. The bonded interactions consists of bond-stretch(E_B, two body), bond-angle bend(E_A, three-body), dihedral angle torsion(E_T, four-body) and improper or inversion term(E_I, four-body)

$$E_b = E_B + E_A + E_T + E_I \tag{2.15}$$

while the non-bonded term consists of van der Waals(E_{vdw}), electrostatic(E_Q, and explicit hydrogen bond terms(E_{hb}) terms

$$E_{nb} = E_{vdw} + E_Q + E_{hb} \tag{2.16}$$

We will use this potential energy equation for all of our Force Fields and will mention it when the the functional form of the energy differs from the conventional one. All the bond-stretching terms are of the form of simple harmonic oscillator

$$E_B = \sum_{bonds} K_r(r - r_0)^2 \tag{2.17}$$

Where r is the distance between atoms and r_0 is the equilibrium distance. Same goes with angle bending term also which has harmonic form

$$E_A = \sum_{angles} K_\theta(\theta - \theta_0)^2 \tag{2.18}$$

where θ is the angle between bonds and θ_0 is the equilibrium angle. While all FFs employ a simple Fourier expansion to represent the dihedral energy, we observe some variation in the assignment of that energy. We will discuss these differences in the section where we compare various available forcefields. Generally, the Improper term in FFs is harmonic which arises out of vibrational nature of the system and is added to enforce the planarity of aromatic rings and other conjugated systems. Generally, Improper term is of the form,

$$E_I = \frac{1}{2}K(\psi - \psi_0)^2 \tag{2.19}$$

where ψ is the angle between bond and the plane and ψ_0 is the equilibrium angle. Almost in all FFs, the non-bonded terms(pairwise terms) have Lenard-Jones and Coulombic form.

$$E_{nb} = \sum_{i<j} [\frac{A_{ij}}{R_{ij}^{12}} - \frac{B_{ij}}{R_{ij}^{6}} + \frac{q_i q_j}{\epsilon R_{ij}}] \tag{2.20}$$

Where A_{ij} and B_{ij} are constants, R_{ij} is the distance between atoms i & j, q_i & q_j are the charges on the the atoms i & j and ϵ is the dielectric constant. In appendix A, I have discussed few commonly used force fields. In the following paragraphs, I have compared some of them by their estimation of physical properties and which fares better.

CHARMM validates charges using empirical fits to interaction energy while OPLS does it by using Monte Carlo(MC) simulations on condensed phase liquids. While CHARMM validates VDW parameters from crystal data while OPLS validates them from liquid simulations[16][17][18]. The OPLS specifies value for A & B, the repulsive and attractive coefficients, respectively whereas CHARMM specifies value for $R^\star$ and ϵ(where $A = \epsilon R^{\star 12}$ and $B = 2\epsilon R^{\star 6}$).

Although all of these FF have simple Fourier expansion to represent dihedral energy, OPLS and AMBER distributes the energy equally among equivalent bond paths (like nine HC-CT-CT-CT-HC dihedrals in ethane) while in CHARMM, the dihedral energy is assigned to only one specific bond path(quartet of atoms).

For hetero-nuclear interactions, OPLS determines the values of A & B using geometric mean combining rules while CHARMM uses arithmetic mean combining rule for $R_\star$ and geometric mean combining rule for ϵ.

The CHARMM94 parameters reproduced the density and heat of vaporization for butane with an average error of 3.2% and 4.5 % while AMBER got the average errors as 1.7 % and 3.0 % and OPLS got 0.9 % and 1.7 %[14]. The CHARMM94 is more complex as it uses different $R^\star$ and ϵ for CH_2 and CH_3 carbons.

As evident from the above results, OPLS provides lowest overall error for the systems mentioned above but this this has been achieved at the expense of fitting the "neat" liquid properties of methane. However, the author[14] concludes that OPLS is appropriate and effective model for studying organic molecules in condensed phase.

We have used OPLS-AA as a Force Field(FF) to model Oil, Phenol and Alkyl-Phenol molecules while Water molecules has been modeled using TIP3P. All the Lennard-Jones co-efficients, bond stretching co-efficients, angle bending co-efficients and, torsional co-efficients for these species have been tabulated in Table 2.1, 2.2, 2.3 and 2.4, respectively. All the force field parameters have been selected from the Jorgenson database of OPLS-AA parameters(2006)(obtained through private communication). The functional form of the potential term in OPLS-AA FF can be written as:

E = $\sum_{bonds} K_r(r - r_0)^2 + \sum_{angles} K_\theta(\theta - \theta_0)^2 + \sum_{i<j} [\frac{A_{ij}}{R_{ij}^{12}} - \frac{B_{ij}}{R_{ij}^{6}} + \frac{q_i q_j}{\epsilon R_{ij}}] +$
$\sum_i \frac{V_1^i}{2}[1 + cos(\phi_i + f_1)] + \frac{V_2^i}{2}[1 - cos(2\phi_i + f_2)] + \frac{V_3^i}{2}[1 + cos(3\phi_i + f_3)]$

Where r is the distance between atoms, r_0 is the equilibrium distance, θ is the angle between bonds, θ_0 is the equilibrium angle, A_{ij} and B_{ij} are constants, R_{ij} is the distance between atoms i & j, q_i & q_j are the charges on the the atoms i & j, ϵ is the dielectric constant, ϕ_i is the dihedral angle, V_1, V_2 and V_3 are the coefficients in the Fourier series, and f_1, f_2 and f_3 are phase angles which are all zero for n-alkanes.

Table 2.1: **OPLS-AA Nonbonded Parameters for n-alkanes, Water, Phenol & Nonyl-phenol**

Atom Type	q(e)	$\sigma(\dot{A})$	ϵ(Kcal/mol)	Atom description
OW	-0.8340	3.150	0.152	Oxygen atom of water molecule
HW	0.4170	0.000	0.000	Hydrogen atom of water molecule
CT(CH3)	-0.1800	3.500	0.066	CH3 carbon atom in alkyl chain
CT(CH2)	-0.1200	3.500	0.066	CH2 carbon atom in alkyl chain
HC	0.0600	2.500	0.030	Hydrogen of carbon atom in alkyl chain
CA	-0.1150	3.550	0.070	Carbon atom in the benzene ring
HA	0.1150	2.420	0.030	Hydrogen atom in the benzene ring
OH	-0.6351	3.070	0.170	Oxygen of the Phenol group
HO	0.4286	0.000	0.000	Hydrogen of the Phenol group

Table 2.2: **OPLS-AA Bond-stretching parameters for n-alkanes, Water, Phenol & Nonyl-phenol**

Bond	K_r(Kcal/mol$^{-1}\dot{A}^2$)	$r_0(\dot{A})$
OW-HW	529.60	0.9572
CT-CT	268.00	1.5290
CT-HC	340.00	1.0900
CA-CA	469.00	1.4000
CA-HA	367.00	1.0800
CA-OH	450.00	1.3640
HO-OH	553.00	0.9450
CA-CT	317.00	1.5100

2.3.2 Long-range Summation Method

Typically simulations involves large systems and as many as 10^5 atoms in the system. Computationally, the most expensive portion of these MD simulations is to calculate long-range interactions as they scales as N^2. So as the number of charges in a system increases, the number of Coulombic interactions grows as the square of that number, potentially resulting in a enormously large number of interactions to calculate.In early implementations of MD simulations, a cut-off was applied which was known as spherical truncation. All the interactions beyond that cut-off were ignored. But this abrupt introduction of cut-off caused system to have energetic discontinuity and resulted in an unstable simulation[20]. Below we discuss some of the modern and computationally efficient strategies used to calculate long range interactions.

If we truncate potential at a distance r_c , the contribution from the tail of the potential u(r) can be written as:

$$u_{tail} = \frac{N\rho}{2} \int dr u(r) 4\pi r^2 \tag{2.21}$$

Where ρ is average number density. Above equation shows that tail correction

Table 2.3: **OPLS-AA Angle-bending parameters for n-alkanes, Water, Phenol & Nonyl-phenol**

Angle	K_θ(Kcal/mol$^{-1}\dot{A}^2$)	θ_0(deg)
HW-OW-HW	34.05	104.52
CT-CT-HC	37.50	110.70
HC-CT-HC	33.00	107.80
CT-CT-CT	58.35	112.70
CA-CA-CA	63.00	120.00
CA-CA-HA	35.00	120.00
CA-CA-OH	70.00	120.00
CA-OH-HO	35.00	113.00
CA-CT-HC	35.00	109.50
CA-CT-CT	63.00	114.00

Table 2.4: **OPLS-AA Fourier Coefficients (kcal/mol) for Torsional Energy Functions.**

System	Dihedral	V_1	V_2	V_3
n-alkanes	CT-CT-CT-HC	0.000	0.000	0.300
	HC-CT-CT-HC	0.000	0.000	0.300
	CT-CT-CT-CT	1.300	-0.050	0.200
Alkyl-phenols	??-CA-CA-??	0.000	7.250	0.000
	HO-OH-CA-CA	0.000	1.682	0.000
	HC-CT-CT-CA	0.000	0.000	0.462
	CT-CT-CA-CA	0.000	0.000	0.000
	HC-CT-CA-CA	0.000	0.000	0.000
	HA-CA-CT-HC	0.000	0.000	0.000

to the potential energy diverges unless potential energy u(r) decays faster than r^{-3}. As tail correction for these long-range interactions diverges, we apply few methods to overcome this like Ewald summation method which makes use of fast convergence obtained by splitting the electrostatic interaction sum into direct space and reciprocal space sums to treat all electrostatic interactions in periodic systems.

Another grid based method i.e.Smooth Particle Mesh Ewald(SPME) summation method (another variant of it is Particle-Particle Particle Mesh Ewald summation method(PPPM)), is being used extensively in scientific fraternity. It minimizes the computational expense of Ewald method and making it of comparable speed with atom truncation methods.

Ewald method:

In Ewald method, We assume that every particle i with charge q_i is surrounded by a diffuse charge distribution such that total charge of this cloud exactly cancels qi so electrostatic potential due to particle i is due to the fraction of q_i that is not screened which at large distance rapidly goes to 0.

In order to correct for the screened charged cloud , we add a compensating

charge cloud(in Gaussian form) which is smoothly varying periodic function and can be represented by a rapidly converging Fourier series[21]. It can be visualized by a diagram given in Fig. 2.11.

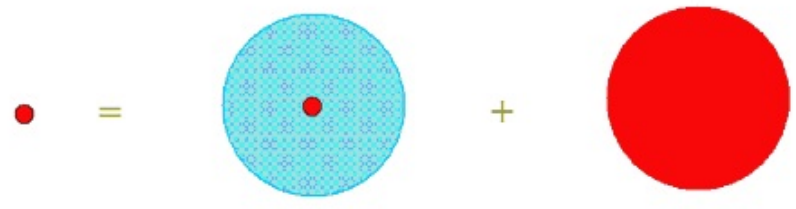

Figure 2.11: **Particle i with charge q_i is surrounded by a diffuse charge distribution(blue) and to correct for the screened charged cloud, adding a compensating charge cloud(red)**

To compute energy of a given charge distribution $\rho(r)$, we can write Poisson's equation of the form:

$$-\bigtriangledown^2\phi(r) = 4\pi\rho(r) \tag{2.22}$$

Where $\rho(r)$ is the electrostatic potential at point r. By accounting for the all three terms i.e. Fourier part of Ewald sum, Correction of self-interaction $\&$ real space sum , we get the expression of the electrostatic contribution to the potential energy which corrects for the long-range interactions in our MD simulations.

SPME/PPPM method:

In many applications , we not only have long-range interactions but short-range interactions as well so it is convenient to use same cut-off radius for real space sum in Ewald summation as for the short-range interactions. As for a fixed cut-off, Fourier part of the Ewald summation scales as $O(N^2)$, we need a different method. We can speed up our long-range calculations by solving Poisson equation for which charges are distributed on mesh. This method was developed by Hockney and Eastwood [1981] originally known as Particle-Particle Particle-Mesh(PPPM) summation method. In this method, the charges in the systems were interpolated on a grid to arrive at a discretized Poisson equation which can be solved efficiently using Fast Fourier Transform(FFT).

Using SPME/PPPM gives much faster Fourier part calculations and it scales as $O(NlogN)$ with system size. Hence in our study, we have used PPPM method in LAMMPS to calculate long range interactions.

2.3.3 Convergence studies for various MD parameters

our attempts to obtained appropriate values for the running parameters used in the MD simulations. Some examples are simulation timestep, bin size

In this section, we have discussed our attempts to obtained appropriate values for the running parameters used in the MD simulations. Some examples are LJ cut-off, MD simulation timestep, bin size used in stress profile calculations. We have also compared two MD engines namely LAMMPS and Culgi in order to pick out the most efficient engine for our calculations.

We have used the cross-sectional area of 64×64 $\dot{A}^2$ as each of the interfacial dimensions is longer than twice the lenght of the alkanes used. We have also used box length across the interface close to 85 $\dot{A}$ by which one can get more atoms in each bin for density profile calculation which smooths out our density profiles by more averaging.

Lennard-Jones cut-off:

We have used LJ cut-off int he range 9 $\dot{A}$ to 12 $\dot{A}$. We compared this with experimental density and conclude that 11 $\dot{A}$ is certainly best suited for this FF. This is in agreement with n-alkane literature comparing density as mentioned in Table 2.5 and results in uniform density profile across simulation box, when the box contains only hydrocarbon molecules. [19]

Table 2.5: **Predicted Dodecane density from various LJ cut-off**

LJ cut-off($\dot{A}$)	Simulation density(gm/cm^3)	Experimental density(gm/cm^3)	Error(%)
9	0.713	0.740[26]	3.6
11	0.736	0.740[26]	0.5
12	0.766	0.740[26]	3.5

MD simulation timestep:

Both 0.5 fs and 1.0 fs MD time-step provides us the appropriate dodecane density as mentioned in Table 2.6. But being conservative, we have used 0.5 fs due to our force field being all atom.

Table 2.6: **Dodecane density from various MD time-steps**

MD time-step(fs)	Simulation density(gm/cm^3)	Experimental density(gm/cm^3)
0.5	0.736(0.004)	0.740[26]
1.0	0.739(0.017)	0.740[26]

Bin size used in stress profile calculations:

In the calculation of IFT, we divide the MD box into smaller bins. Binnning is a method to calculate properties of a simulation box by dividing the box into small boxes along one axis. We then time average the properties across all bins and predict them. Stree profile is calculated independently in each bin along the direction perpendicular to the interface. This provides a stress profile curve for the box, averaged over the duration of the MD run. Bin size used to generate stress profile determines the accuracy of the calculations. We varied the bin size in the range 0.1 - 2.0 $\dot{A}$. We found the size 0.15 $\dot{A}$ to be suitable for accurate predictions as can be seen in Fig. 2.12. We have discussed the calculation of IFT and stress profile in greater detail in Section 3.

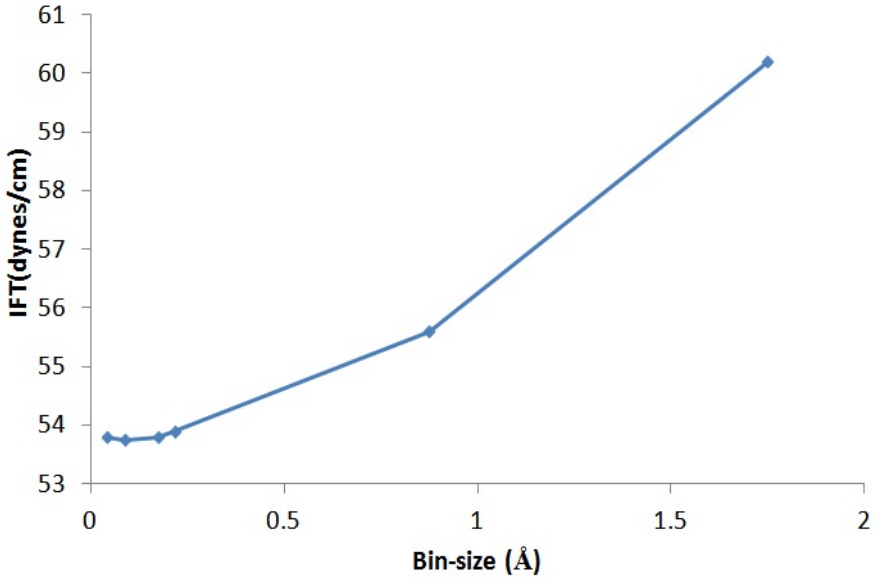

Figure 2.12: **IFT values as a function of bin size for Dodecane-Water simulation box**

Comparison of two MD engines:

We evaluated two MD engines available in open domain, namely LAMMPS and Culgi. While Culgi is a commercial software, LAMMPS is a free open source package developed in Sandia National Labs. To compare the computational efficiency from both these MD engines, we carried out a test simulation which had water molecules. We ran MD on both LAMMPS and Culgi with TIP3P as a Force Field(FF), NPT ensemble, room temperature and Pressure taking 1500 atoms with box-size 30 $\dot{A}$ each in each of the 3 dimensions. The NPT MD simulation was carried out for 10 ps and had SPME/PPPM accuracy of 0.0001 Kcal/mol. We ran these simulations on Westmere based HPC clusters, using multiple cores per node. Table 2.7 provides a comparison of various combinations.

Table 2.7: **Run-times from both MD engine, Culgi and LAMMPS for the NPT MD simulation of pure water box**

Number of cores(n)	Run-time on Culgi(s)	Run-time on LAMMPS(s)	Ratio
1	5801	215.83	26.9
2	3767	118.7	31.7
4	1978	65.14	30.4

As evident from the Table 2.7, LAMMPS fares better than Culgi in terms of computational time needed to do same MD calculation. Based on these results, we selected LAMMPS for our research.

Chapter 3

Stress Profile Calculation

Surface tension is the contractile nature of a liquid with which it tries to minimize it's surface area. If water is placed in the contact with oil, the interface between the two immiscible and dissimilar liquids will have contractile tendency too. This results from the greater cohesive interactions between water-water and oil-oil molecules than adhesive interactions between water-oil molecules. Several Industrial processes encounter liquid-liquid systems which come together at some stage to form an interface. The physical behavior of these interactions are understood by analyzing stress profiles and are quantified by the inter-facial values of these systems.

We have investigated stress profile across interfacial surface as we are trying to minimize the IFT values. Stress profile calculation in LAMMPS is done via a in-built compute named "stress/atom" which provides summed up values of all stress tensor components for a particular bin. Kirkwood-Buff formalism is used in literature to a great extent, to calculate interfacial properties at liquid-liquid interface. This formalism is briefly described below[22][23].

We can calculated lateral pressure profile along the box across the interface using it's mechanical definition:

$$p(x) = \sigma_T(x) - \sigma_N(x) \tag{3.1}$$

Which can also be written as:

$$p(x) = \sigma_T(x) - \sigma_{xx}(x) \tag{3.2}$$

where,

$$\sigma_T(x) = \frac{\sigma_{yy}(x) + \sigma_{zz}(x)}{2} \tag{3.3}$$

and x is the direction normal to the bilayer. Here σ_N and σ_T are normal and tangential components of stress tensor at the the Oil-Water interface. Both of them are same in bulk and have difference across the interface because of the anisotropy of the structures at the interface. We calculate IFT by taking their difference across a surface.

$\sigma_T(x)$ and $\sigma_N(x)$ were calculated from each slab of the simulation box during the simulation as a time average by the Kirkwood-Buff theory in MD as follows:

$$\sigma_N(x) = \rho(x)K_BT - \frac{1}{V_{slab}}\langle\sum_{i,j}\frac{x_{ij}^2}{r_{ij}}\frac{du(r_{ij})}{r_{ij}}\rangle \tag{3.4}$$

$$\sigma_T(x) = \rho(x)K_BT - \frac{1}{V_{slab}}\langle\sum_{i,j}\frac{(y_{ij}^2+z_{ij}^2)}{2r_{ij}}\frac{du(r_{ij})}{r_{ij}}\rangle \tag{3.5}$$

where V_{slab} is the slab volume, $\rho(x)$ is the density of the slab, K_B and T are Boltzmann constant and absolute temperature. Angle bracket shows the ensemble average of all atoms located in the slab at x. r_{ij}, x_{ij}, y_{ij} and z_{ij} are the distances between atoms and it's components whereas $u(r_{ij})$ is the potential energy for the atomic pair i and j.

To calculate IFT across Oil-Water interface, we can use:

$$\gamma = -\frac{1}{2}\int p(x).dx \tag{3.6}$$

Which is the area under the curve of stress profile along x-axis. The IFT values has been reported in the units of dynes/cm throughout this document.

Chapter 4

Details of Simulations

DPD Simulations

We have calculated interfacial prpoerties for three n-alkanes i.e. Hexanee, Nonane and Dodecane as a Oil. We have used box-size of about 83×64×64 $\dot{A}^3$ having interface perpendicular to the x direction for doing DPD simulations which has bead density of 3.0 beads/grid cell. DPD simulations requires repulsion parameters to do the dynamics(like FF parameters in MD). DPD simulations were carried out for 400 ps with timestep of 0.02 ps.

After DPD simulations, we also do mapping from coarse grained beads to atoms in Culgi itself and then minimize the system using OPLS-AA before converting the box to LAMMPS input file. This file is used by LAMMPS to do MD calculations.

MD Simulations

The systems has been used post mapping by first minimizing the box and then run NPT MD, NVT equilibration MD and NVT production MD correspondingly. The temperature and pressure has been maintained at 298.15 K and 1 bar by using Berendson thermostat and barostat in all these calculations. We have used the all atom potential parameters which is OPLS-AA force field for all of the hydrocarbon molecules and TIP3P original for modelling water molecules for all our MD calculations.

We have used the global cut-off of 11.0 $\dot{A}$ for van der Waals interactions. Smooth particle-mesh Ewald summation(SPME/PPPM) has been used to calculate long-range electrostatic interactions having accuracy of 0.0001 which is unitless as it is desired relative error in forces. The output co-ordinates have been calculated at every 1.0 ps for each MD having a timestep of 0.5 fs. The box has been simulated for 5 ns with NPT simulation(iso-interfacial area) and was rescaled after NPT simulation by averaging box side lengths by doing another NPT simulation for 20 ps. NVT equilibration MD for 500 ps were done before NVT production run for 3 ns was carried out.

The Stress profile has been calculated by averaging lateral stress as an output every 100 steps during NVT production run for a bin size of about 0.15 $\dot{A}$. Composition of various systems has been given in the Table 4.1.

We tried different combinations of Phenol-Oil-Water molecules to investigate

Table 4.1: **Composition of n-alkane-water systems used in simulations**

	Water molecules	Oil molecules
Hexane-Water	5850	975
Nonane-Water	5850	650
Dodecane-Water	5856	487

these surfactant(Phenol or Alkyl-Phenols)-Oil-Water systems. All the Phenol(or Alkyl-phenols) molecules had been placed in the bulk Oil at the start of the simulations. We have varied the phenol concentration from 0.05 mol fraction to 0.25 mol fraction. The n-alkanes studied are Nonane and Dodecane. The compositions for these Phenol-Oil-Water systems has been reported in Table 4.2 and 4.3.

These tables are also applicable for Nonyl-Phenol in place of phenol i.e. Nonyl-Phenol-Oil-Water and Phenol-Oi-Water will have same composition if the concentration of the surfactant is same. Here, the concentration of Phenol has been defined as the mol fraction of phenol molecules in the Oil bulk.

Table 4.2: **System composition for various Phenol concentrations in Nonane-Water**

Phenol Concentration	Nonane molecules	Water molecules	Phenol molecules
0	650	5850	0
0.05	616	5952	34
0.08	598	6006	52
0.15	553	6141	97
0.25	488	6336	162

Table 4.3: **System composition for various Phenol concentrations in Dodecane-Water**

Phenol Concentration	Dodecane molecules	Water molecules	Phenol molecules
0	487	5856	0
0.05	462	6006	25
0.08	448	6090	39
0.15	415	6288	72
0.25	366	6582	121

The DPD part of the protocol has been performed in Chemistry Unified Language Interface(Culgi) which is a third party propriety software while MD part has been done in Large-scale Atomic/Molecular Massively Parallel Simulator(LAMMPS) which is open source code for running MD simulations. All the visualizations has been done using Visual Molecular Dynamics(VMD).

Chapter 5

Results and Discussion

5.1 Validation of FF

We carried out DPD and MD simulations on Oil-Water to validate our methods and to confirm the applicability of OPLS-AA as a Force Field(FF) to these systems for calculating properties like Interfacial Tension(IFT).

5.1.1 Density

We have validated the densities of these pure n-alkane systems at normal temperature and pressure, with available experimental data. We did simulations on pure Oil and pure Water systems to get the densities using the protocol mentioned in section "Details of Simulations". The density profiles and density values of the pure systems are shown with comparison with the experimental ones in Fig. 5.1 and Table 5.1 given below.

Table 5.1: **Densities of n-alkanes and Water at NPT**

	Simulation Density(gm/cm^3)	Exp. Density(gm/cm^3)	Error(%)
Hexane	0.63	0.65[24]	4
Nonane	0.69	0.71[25]	2.4
Dodecane	0.73	0.74[26]	0.6
Water	1.015	1.001[27]	1.4

The densities are within 2.5 % of the experimental ones for higher molecular weight n-alkanes which shows the applicability of OPLS-AA to the these n-alkane systems. The spatial density profiles for the Dodecane-Water and Nonane-Water systems are shown in Fig. 5.2 and 5.3 below.

As one can observe that the middle of the box is filled with Oil while the rest of it is filled with Water. The distribution of Oil and Water is uniform which reflects in flat spatial density profiles. The fluctuations in density in the bulk for both Oil and Water are within 1 % which shows that the systems have equilibrated.

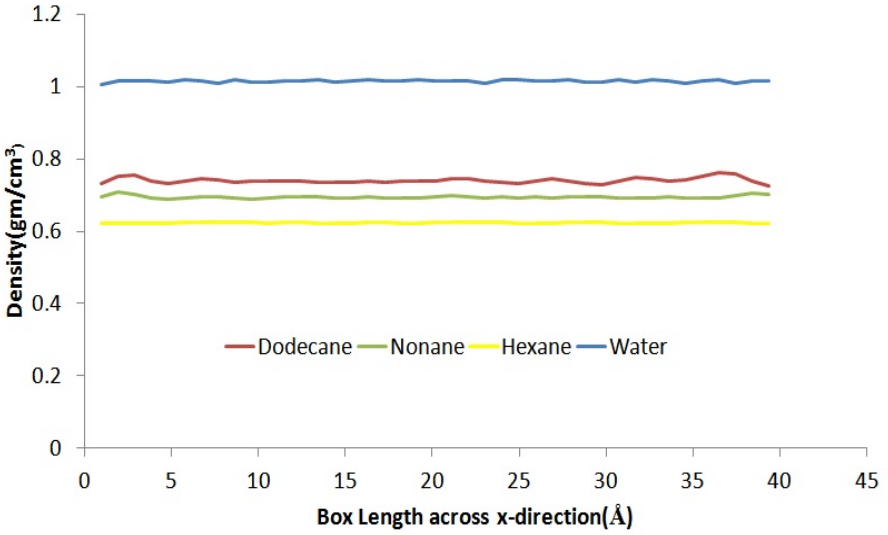

Figure 5.1: **Predicted densities from MD simulations, along the length of MD box, for bulk simulations of dodecane, nonane, hexane and water.**

5.2 Validation of Protocol for IFT

Lateral stress profiles has been calculated using a built-in code in LAMMPS by Kirkwood-Buff formalism(described in the "Theory" section in detail). The comparison of Stress profiles for Nonane-Water and Dodecane-Water system has been shown in Fig. 5.4.

Interfacial Tension(IFT) values can be calculated by integrating the stress profile curve across the interface. As Dodecane has higher molecular weight than Nonane and Hexane, it repels Water much more and that shows in the IFT values. It should also be evident from the Fig. 5.4 that the area under the curve will be more for Dodecane than Nonane or Hexane which is the IFT value for that system. The elevation in IFT values with increasing molecular weight of n-alkanes can be observed in Table 5.2.

Table 5.2: **Comparison of experimental and predicted IFT(dynes/cm) for water-alkane systems**

	Predicted IFT	Exp. IFT	Error(%)
Hexane-Water	45.7(+/-0.17)	50.38[28]	9.2
Nonane-Water	50.1(+/-0.75)	51.63[28]	2.9
Dodecane-Water	52.6(+/-1.05)	52.55[28]	0.09

IFT values of Dodecane-Water and Nonane-Water systems shows a good match with the values available in literature. We hope to use these systems for our further investigations.

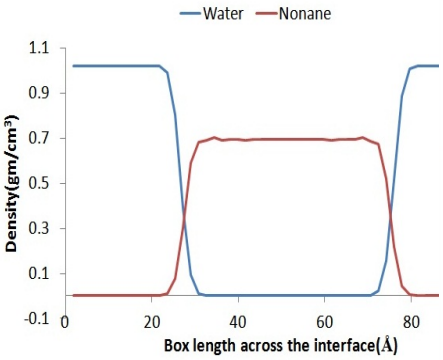

Figure 5.2: **Spatial density profiles of Nonane & Water acorss interface**

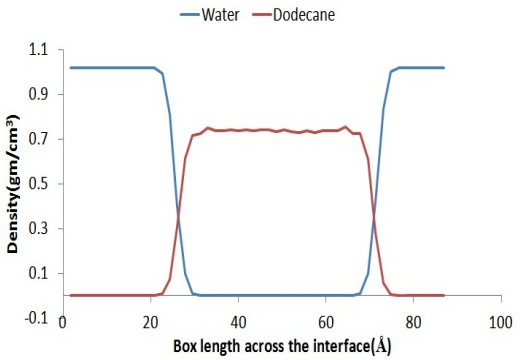

Figure 5.3: **Spatial density profiles of Dodecane & Water acorss interface**

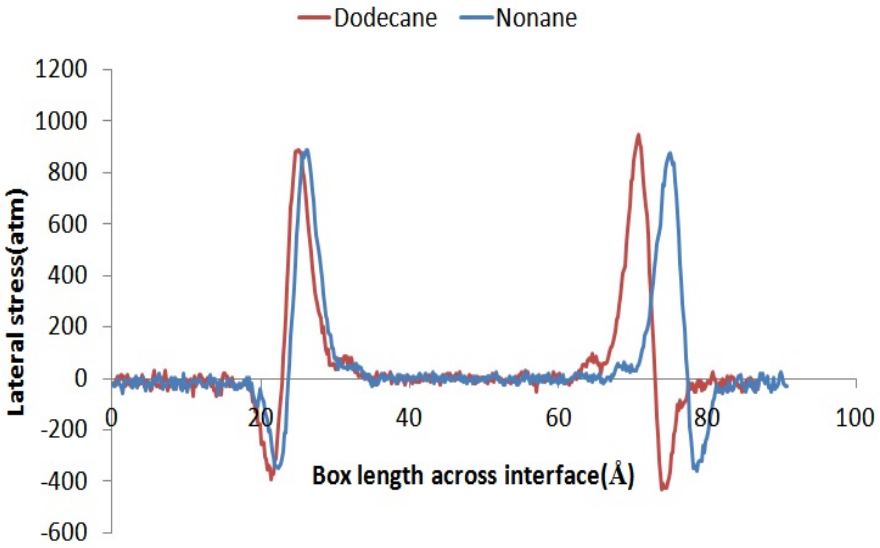

Figure 5.4: **Comparison of lateral stress profiles (Atm) of Nonane-Water and Dodecane-Water acorss the interface**

In a realistic oil reservoir, we encounter tempratures in the range 50-125 C and upto 700 bar pressure. We are trying demonstrate the validity of these methods also for reseroivr conditions. Hence in the following discussion we have compared predicted IFTs with eperimental ones, for elevated pressures and temperatures. The IFT results for 1 bar pressure and different temperatures has been tabulated in Table 5.3 below.

Table 5.3: **Comparison of experimental and predicted IFT(dynes/cm) for water-alkane systems with varying temperature**

	Temperature(degree C)	Predicted IFT	Exp. IFT	Error(%)
Nonane-Water	25	50.1(+/-0.75)	51.63[28]	2.9
Nonane-Water	60	45.2(+/-0.35)	48.82[28]	7.4
Nonane-Water	125	40.1(+/-0.42)	43.35[28]	7.5
Dodecane-Water	25	52.6(+/-1.05)	52.55[28]	0.1
Dodecane-Water	60	48.3(+/-0.64)	50.00[28]	3.4
Dodecane-Water	125	42.4(+/-0.46)	44.87[28]	5.5

Here, the experimental results has been extrapolated by fitting a straight line to the experimental values obtained in this paper[28]. Since IFT doesn't change by a considerable amount due to pressure variation, we did calculations for 125 C at 700 bar as carrying them out at 1 bar will be non-physical(125 C is greater than the boiling point of water).

As noticeable from the Table 5.3, the difference between the IFT values from simulations and experiments widens as we go towards higher temperature. We are able to predict IFT within 10 % of the experimental value for realistic oil reservoir which has temperature range of 25-125 C. In the following sections, we have applied these developed methods to study the effect of Phenol and Nonyl-Phenol on the Oil-Water systems.

5.3 Effect of Phenol on IFT of Oil-Water interface

Here, we will use the methods discussed in previous sections to study the effect of suspected surface active species existing in crude oils. As a first example, we have studied molecules from alkyl-phenol family, suspected to be among surface active components of crude oils. To demonstrate the surface effectiveness, we have started out by adding simple phenol to oil-water systems before moving on to the alkyl-phenols.

In the Fig. 5.5, we have compared stress profiles for two systems which are (a) Nonane-Water and (b) Nonane-Water with 0.15 mol fraction of Phenol. Here, the lateral stress profile has been plotted across the x-axis which is the axis perpendicular to the interface.

It is clear from the above plot that the addition of phenol in the Oil-Water system, has not only reduced the peaks in the stress profile but also decreased the area under the curve which is the IFT of the system. This accounts for the surface effectiveness of the phenol molecules on the oil-water interface. We have tabulated the effect of phenol on the IFT value in oil-water system taking oil as both Nonane and Dodecane in Table 5.4.

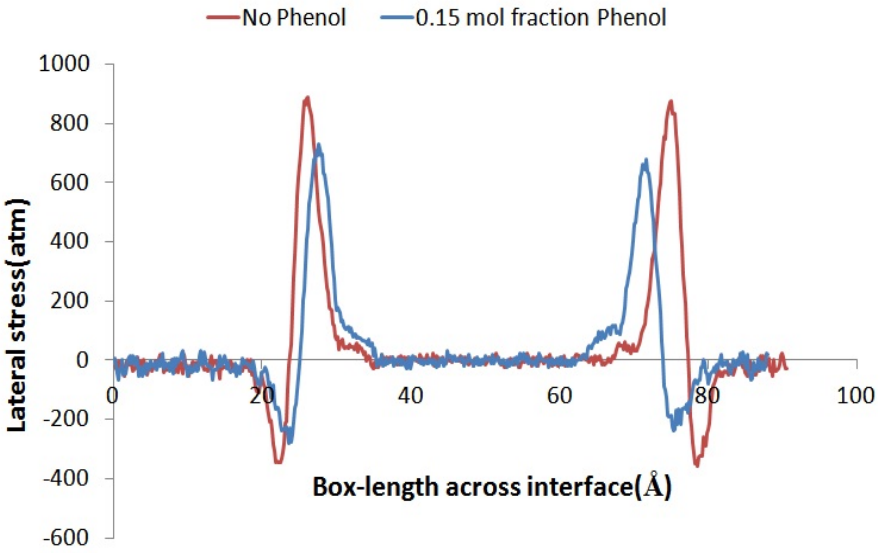

Figure 5.5: **Lateral Stress profile (Atm) for Nonane-Water box with no phenol(red curve) and with 0.15 mol fraction Phenol(blue curve). It is indicating lowered interfacial stress with addition of phenol to the Nonane-Water interface.**

Here, the predicted IFT values has been reported in dynes/cm and has standard deviation value from 3 independent runs in the bracket adjacent to it. This Table shows the reduction in the predicted IFT values with addition of more and more Phenol in both Nonane-Water and Dodecane-Water system. The IFT values also maintains the "rank order" for Nonane and Dodecane within the concentrations of phenol studied. Here, the "rank order" is defined is the order in the values of IFT with the number of carbon atoms in the oil specie.

Table 5.4: **Predicted IFT (dynes/cm) of Phenol-Oil-Water system with varying Phenol concentrations**

Phenol Concentration(%)	IFT with Oil=Nonane	IFT with Oil=Dodecane
0	50.1(+/-0.75)	52.6(+/-1.05)
0.5	49.1(+/-0.21)	52.5(+/-0.92)
0.08	47.2(+/-1.22)	51.8(+/-0.49)
0.15	44.5(+/-0.21)	48.1(+/-0.07)
0.25	36.1(+/-1.6)	43.7(+/-1.48)

5.4 Effect of Alkyl-Phenols on IFT of Oil-Water interface

In this section, we have discussed the effect of Alkyl-Phenols on the Oil-Water system. Alkyl-Phenols are non-ionic surfactants which can be classified as good interfacial tension reducer and wetting agent. They are amphiphilic in nature i.e. they have both hydrophobic and hydrophilic groups in them.

Here, we have taken Nonane as oil and Nonyl-Phenol as alkyl-phenol for our investigations. We have used 3 isomers of Nonyl-Phenol which are (a) para-linear Nonyl-Phenol molecule, (b) para-branched Nonyl-Phenol molecule and (c) ortho-linear Nonyl-Phenol molecule. The structures of these isomers are shown in Fig. 2.6, 2.7 and 2.8. We have chosen these 3 isomers because while (a) has small head size and long linear tail length, (b) has small head size but bulkier branched alkyl group as tail and, (c) has bigger head group(due to alkyl chain being on ortho position) and no tail. These 3 isomers covers both "head size" and "bulky tail" effect of this surfactant(Alkyl-Phenol) on Oil-Water interface. It will clarify the dependence on surfactant's topology on it's surface efficiency on Oil-Water interface.

Fig. 5.6 and 5.7 shows the comparison of the lateral stress profile for para-linear & para-branched Nonyl-Phenol and para-linear & ortho-linear Nonyl-Phenol, respectively. These stress profiles has been plotted across the interface for Nonane-Water box containing Nonyl-Phenol having concentration of 0.25 mol fraction. As mentioned in earlier sections, the concentration of Phenol has been defined as the mol fraction of phenol molecules in the Oil bulk.

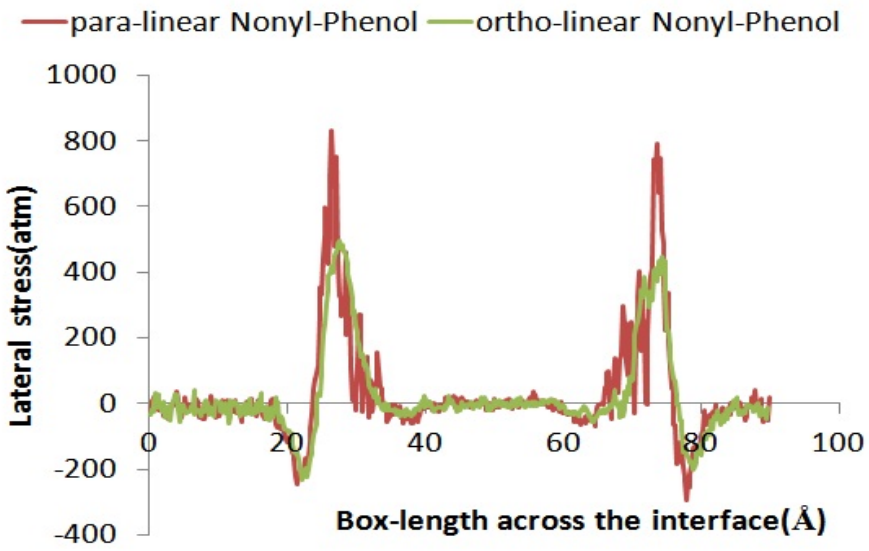

Figure 5.6: **Comparing Lateral Stress profile (Atm) for Nonane-Water box with 0.25 mol fraction para-linear and ortho-linear Nonyl-Phenol in Nonane-Water box.**

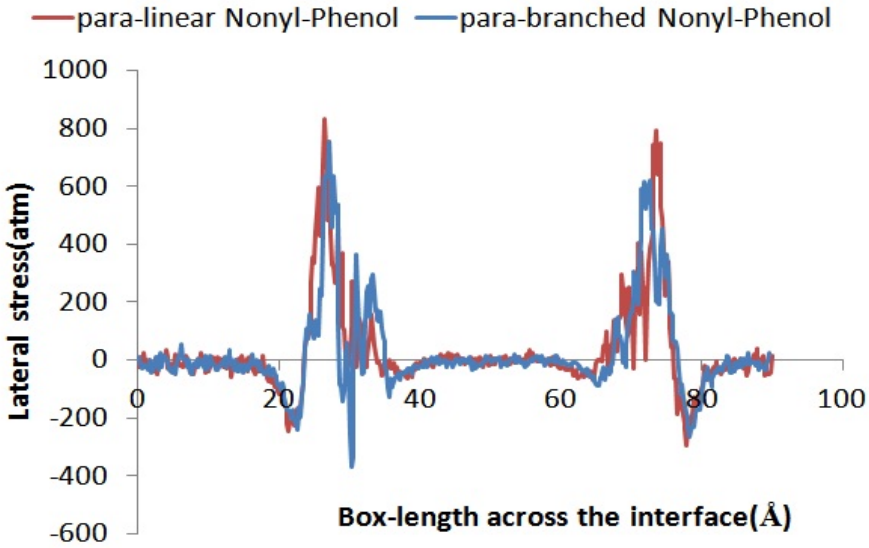

Figure 5.7: **Comparing Lateral Stress profile (Atm) for Nonane-Water box with 0.25 mol fraction para-linear and para-branched Nonyl-Phenol in Nonane-Water box.**

As evident from Fig. 5.6 and 5.7, the stress profiles for the system with para-

linear Nonyl-Phenol seems to have higher peak value than the one with para-branched and ortho-linear Nonyl-Phenol. It is also evident from the IFT values tabulated in Table 5.5 for various different concentrations of these isomers of Nonyl-Phenol.

Table 5.5: **Predicted IFT(dynes/cm) of Nonyl-Phenol-Nonane-Water system with varying Phenol concentrations. Here, Phenol concentration has been defined as the mol fraction of the bulk oil.**

Phenol Concentration	para-linear	para-branched	ortho-linear
0	50.1(+/-0.75)	50.1(+/-0.75)	50.1(+/-0.75)
0.08	44.7(+/-1.38)	43.5(+/-0.28)	43.0(+/-0.85)
0.15	40.0(+/-1.01)	37.4(+/-0.35)	36.1(+/-1.0)
0.25	34.3(+/-1.28)	25.5(+/-0.31)	26.4(+/-1.42)

Here, the predicted IFT values has been reported in dynes/cm and has standard deviation value from 3 independent runs in the bracket adjacent to it. It is clear from the above Table 5.5 that para-branched and ortho-linear Nonyl-Phenols are more efficient as a surface active specie than the para-linear Nonyl-Phenol. Here, the efficiency has been defined as the reduction in the IFT value of the system for a particular concentration of alkyl-phenol in bulk oil.

Nonyl-Phenol being a non-ionic surfactant has both hydrophobic and hydrophilic groups. While the hydrophilic Phenol group will tend to be in the Water phase, the hydrophobic Nonyl chain will be buried inside the bulk oil. It has been schematically depicted in Fig. 5.8.

We have plotted the mass density profiles for Nonane-Water system with 0.15 mol fraction of Nonyl-Phenol in Fig. 5.9, 5.10 and 5.11. The three isomers of Nonyl-Phenol considered are (a)para-linear Nonyl-Phenol, (b)para-branched Nonyl-Phenol and, (c)ortho-linear Nonyl-Phenol. Here, the density profiles has been plotted for Nonane, Water, hydroxyl group of Nonyl-Phenol, Benzene group of Nonyl-Phenol and, Nonyl chain of Nonyl Phenol.

The varying efficiency of the three isomers of Nonyl-Phenol at reducing IFT can be attributed to mainly 2 factors. (a) the head size of Nonyl-Phenol(group towards Water region) and, (b) the tail bulkiness (branching of alkyl chain in Oil region).

The para-linear Nonyl-Phenol has smaller head size than ortho-linear Nonyl-Phenol. The head of para-linear Nonyl-Phenol essentially comprises only the phenol group. The ortho-linear Nonyl-Phenol have bulkier head group due to Nonyl group being attached on the ortho position. The head group in ortho-linear Nonyl-Phenol includes the part from alkyl chain too apart from Phenol group. It can be seen in Fig. 5.9 and 5.11, where the alkyl chain(dark purple curve) of ortho-branched Nonyl-Phenol is on the interface of Oil-Water as compared to the alkyl chain of para-linear Nonyl-Phenol which is well dissolved inside the bulk oil.

The para-linear Nonyl-Phenol also has a longer linear alkyl tail buried inside the bulk oil than para-branched Nonyl-Phenol. It is evident from density profile of alkyl chain (dark purple curve) in para-linear Nonyl-Phenol in Fig. 5.9 as compared to the alkyl chain of para-branched shown in Fig. 5.10. The tail of para-linear Nonyl-Phenol is less bulkier than that of para-branched Nonyl-Phenol due to Nonyl chain being linear instead of branched.

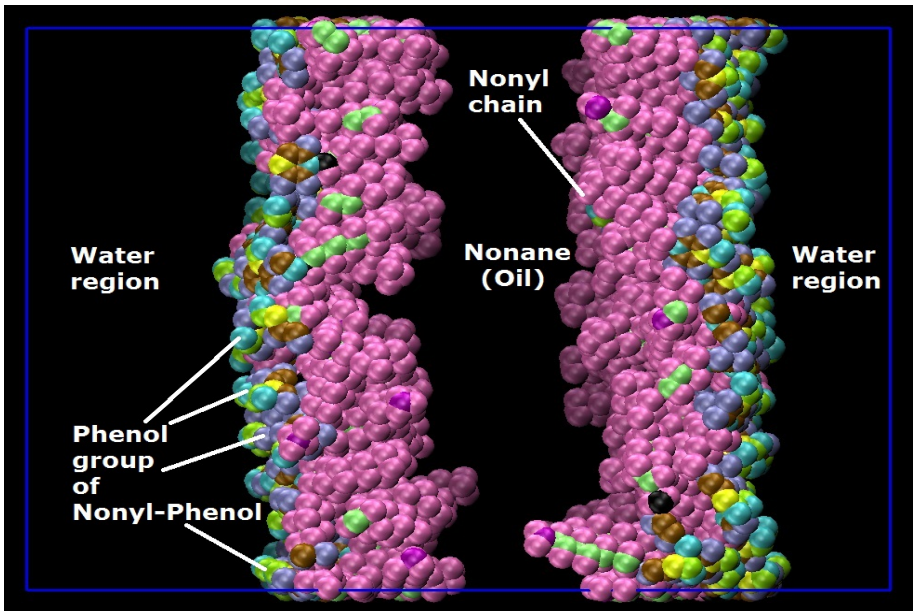

Figure 5.8: **Simulation box with only para-linear nonyl-phenol made visible, nonane and water molecules are not shown. Here, pink spheres shows the Nonyl chain of Nonyl-Phenol at the interface while blue, green, yellow and other colored spheres consists of Phenol group of Nonyl-Phenol molecules. The middle of the box is filled with Nonane molecules(which is between two layers of Nonyl-Phenol) while the rest of it is filled with water(on either side of these layers).**

Due to larger head size in ortho-linear Nonyl-Phenol and tail bulkiness in para-branched Nonyl-Phenol, these species cover more Oil-Water interfacial area than para-linear Nonyl-Phenol. Increasing the size of the head group or increasing the bulkiness of tail group implies increased steric hindrance between surfactants. They require more space and have stronger excluded volume interactions. Their strongly hydrophilic head groups force them into a high-entropy arrangement. This enables these isomers to cover surface area more efficiently (or efficient packing at the interface) which is the reason of lowering in the interfacial tension at the Oil-Water interface.

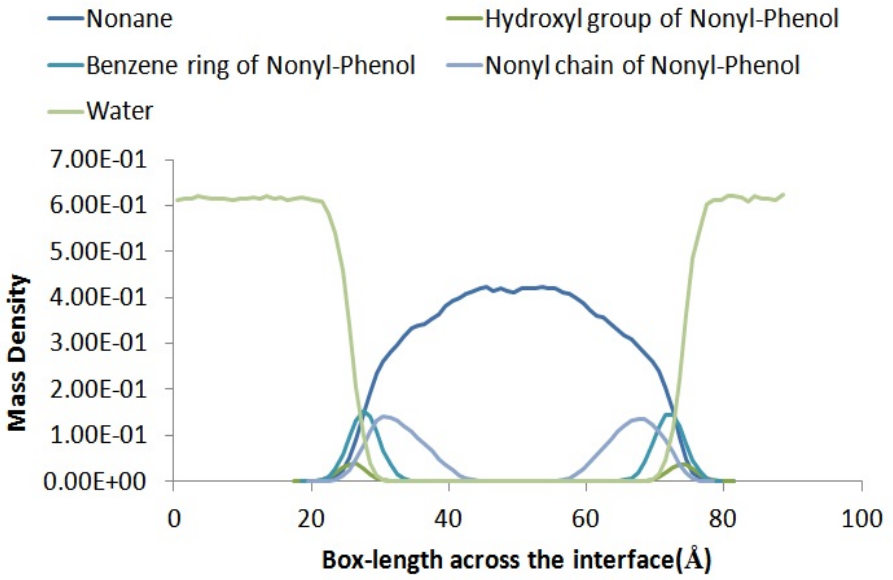

Figure 5.9: **Mass density profile($amu/\AA^3$) for Nonane-Water box with 0.15 mol fraction para-linear Nonyl-Phenol**

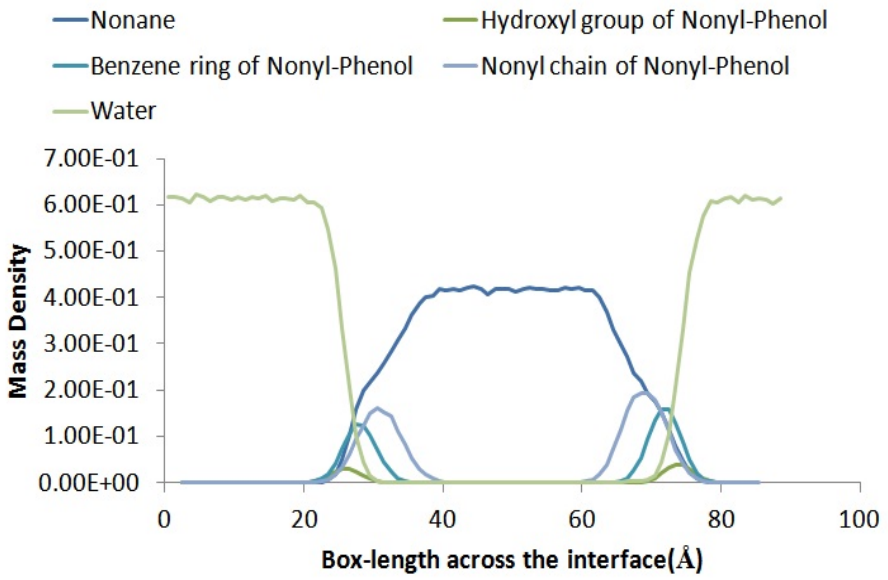

Figure 5.10: **Mass density profile($amu/\AA^3$) for Nonane-Water box with 0.15 mol fraction para-branched Nonyl-Phenol**

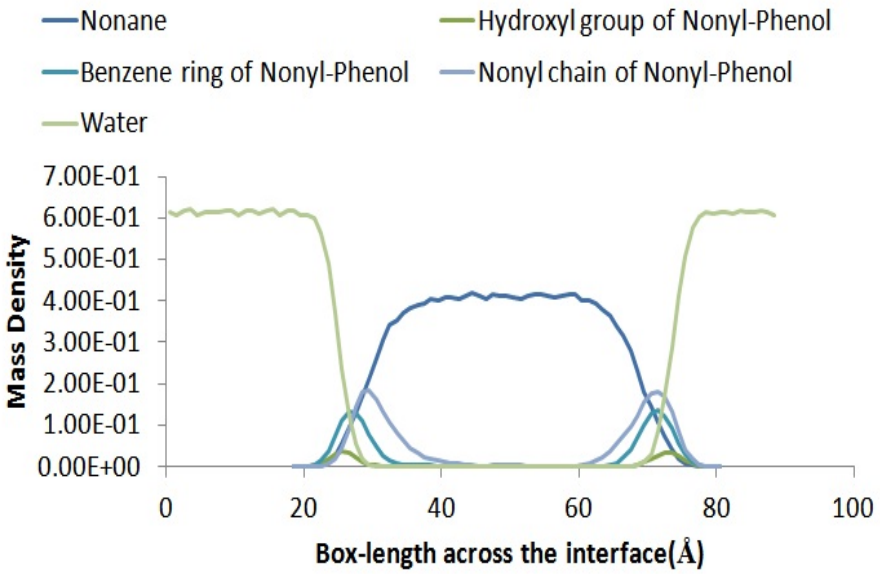

Figure 5.11: **Mass density profile($amu/\dot{A}^3$) for Nonane-Water box with 0.15 mol fraction ortho-linear Nonyl-Phenol**

Chapter 6

Conclusion

In this report, we have started a concerted effort to derive predictive methods for IFT, considering the importance of obtaining accurate estimates of IFT between oil and brine in reservoir conditions. The primary objective of this program is to demonstrate the feasibility of accurate IFT predictions, starting with atomistic models for oils and brine. We have worked with simple oils, namely n-alkanes as validation systems for the first phase of the program. We have screened down protocols for atomistic simulations, the required force fields and molecular models. We now have protocols to predict IFT accurate within about 10% of experimental values. At the same time, the methods also predict density to within 2% of experimental.

After protocol development and validation, we have used them to study the effect of suspected surface active species existing in crude oils, on the IFT of oil and brine. In the first instance, we studied molecules from alkyl-phenol family, suspected to be amongst surface active components of crude oils. We conclude that the alkyl-phenol acts like a natural surfactant and reduces IFT between oil and brine. We have also compared the surface efficiency of 3 different isomers of Nonyl-Phenol molecules as a surfactant. We observed the efficiency of these surfactants by comparing IFT values of the systems with the different concentrations of these surfactants. We conclude that para-branched and ortho-linear Nonyl-Phenol are more efficient at reducing IFT than para-linear Nonyl-Phenol.

In realistic oil reservoir, the recovery of crude oil from oil reservoirs is dependent on the interactions of crude oil, brine, the rock and other chemical species present at the interfaces. In future, these developed methods can be applied to Oil-Brine system instead of Oil-Water systems. We can observe the effects of the salinity on the interfacial behavior on these systems. These methods can also be used to study the relative interactions between various surface active species existing in crude-oils such as asphaltenes, naphthenic acids $\&$ carbazoles.

References

[1] James Sheng, *Modern Chemical Enhanced Oil Recovery : Theory and Practices,* ISBN: 978-1-85617-745-0.

[2] Johannes G. E. M. Fraaije, Kunj Tandon, Shekhar Jain, Jan-Willem Handgraaf , and Marten Buijse, *Method of Moments for Computational Microemulsion Analysis and Prediction in Tertiary Oil Recovery* Langmuir, 2013, 29 (7), pp 2136-2151.

[3] Marten Buijse, Kunj Tandon and Shekhar Jain, Jan-Willem Handgraaf and Johannes G.E.M. Fraaije, *Surfactant optimization for EOR using advanced chemical computational methods,* SPE 154212.

[4] Makoto Kunieda, Kennichi Nakaoka, Yunfeng Liang, Caetano R. Miranda, Akira Ueda, Satoru Takahashi, Hiroshi Okabe, and Toshifumi Matsuoka, *Self-Accumulation of Aromatics at the Oil-Water Interface through Weak Hydrogen Bonding,* J. AM. CHEM. SOC. 2010, 132, 18281-18286.

[5] John W. Dower, *Readings compiled for History 21.479. ,* 1991.

[6] *http://www.kintechlab.com/solutions/methodology/,* Kintech Lab, 1998-2014.

[7] Zhengxia Chen, Xiuli Cheng, Haishi Cui, Ping Cheng, Hongyan Wang, *Dissipative particle dynamics simulation of the phase behavior and microstructure of CTAB/octane/1-butanol/water microemulsion,* Colloids and Surfaces A: Physicochem. Eng. Aspects 301 (2007) 437-443

[8] Zhiqiang Bai, Hongxia Guo, *Interfacial properties and phase transitions in ternary symmetric homopolymerecopolymer blends: A dissipative particle dynamics study,* Polymer 54 (2013) 2146-2157

[9] Alder, B. J.; T. E. Wainwright (1959), *Studies in Molecular Dynamics. I. General Method,* J. Chem. Phys. 31 (2).

[10] A. Rahman (1964), *Correlations in the Motion of Atoms in Liquid Argon,* Phys Rev 136 (2A)

[11] Martin Karplus and Gregory A. Petsko, *Molecular Dynamics Simulations in Biology,* Nature Vol. 347, 18 Oct. 1990

[12] Stewart A. Adcock and J. Andrew McCammon, *Molecular Dynamics: Survey of Methods for Simulating the Activity of Proteins,* Chem. Rev. 2006, 106, 1589-1615

[13] Stephen L. Mayo, Barry D. Olafson, and William A. Goddard III, *DREIDING: A Generic Force Field for Molecular Simulations,* J. Phys. Chem. 1990, 94, 8897-8909

[14] Wendy D. Cornell, Piotr Cieplak, Christopher I. Bayly, Ian R. Gould, Kenneth M. Merz, Jr. David M. Ferguson, David C. Spellmeyer, Thomas Fox, James W. Caldwell, and Peter A. Kollman, *A Second Generation Force Field for the Simulation of Proteins, Nucleic Acids, and Organic Molecules,* J. Am. Chem. SOC. 1995, 117, 5179-5197

[15] J. Wang, P. Cieplak and P. A. Kollman, *How Well Does a Restrained Electrostatic Potential (RESP) Model Perform in Calcluating Conformational Energies of Organic and Biological Molecules? ,* J. Comput. Chem. 21, 1049-1074 (2000)

[16] Alexander D. MacKerell, Jr. Nilesh Banavali, Nicolas Foloppe, *Development and Current Status of the CHARMM Force Field for Nucleic Acids,* 2001 John Wiley & Sons, Inc. Biopoly (Nuvleic Acid Sci) 56: 257-265, 2001

[17] A. D. MacKerell, Jr. D. Bashford,, M. Bellott, R. L. Dunbrack, Jr., J. D. Evanseck, M. J. Field, S. Fischer, J. Gao, H. Guo, S. Ha, D. Joseph-McCarthy, L. Kuchnir, K. Kuczera, F. T. K. Lau, C. Mattos, S. Michnick, T. Ngo, D. T. Nguyen, B. Prodhom, W. E. Reiher, III, B. Roux, M. Schlenkrich, J. C. Smith, R. Stote, J. Straub, M. Watanabe, J. WioÂťrkiewicz-Kuczera, D. Yin,Âğ and M. Karplus, *All-Atom Empirical Potential for Molecular Modeling and Dynamics Studies of Proteins,* J. Phys. Chem. B 1998, 102, 3586-3616

[18] William L. Jorgensen, David S. Maxwell, and Julian Tirado-Rives, *Development and Testing of the OPLS All-Atom Force Field on Conformational Energetics and Properties of Organic Liquids,* J. Am. Chem. Soc. 1996, 118, 11225-11236

[19] MELISSA L. P. PRICE, DENNIS OSTROVSKY, WILLIAM L. JORGENSEN, *Gas-Phase and Liquid-State Properties of Esters, Nitriles, and Nitro Compounds with the OPLS-AA Force Field,* Journal of Computational Chemistry, Vol. 22,

No. 13, 1340-1352 (2001)

[20] Abdulnour Y. Toukmaji, John A. Board Jr., *Ewald summation techniques in perspective: a survey,* Computer Physics Communications 95 (1996) 73-92

[21] Essmann U et al, *A smooth particle mesh Ewald method,* J. Chem. Phys. 103 8577 (1995)

[22]] R. Goetz and R. Lipowsky, *Computer simulations of bilayer membranes: Self-assembly and interfacial tension,* J. Chem. Phys., 108:7397âĂŞ7409, 1998

[23] Pier Luigi Luisi, Peter Walde, *Giant Vesicles: Perspectives in Supramolecular Chemistry ,*

[24] Eulogio JimÃĺnez, Herminio Casas, Luisa Segade, and Carlos Franjo, *Surface Tensions, Refractive Indexes and Excess Molar Volumes of Hexane + 1-Alkanol Mixtures at 298.15 K ,* J. Chem. Eng. Data 2000, 45, 862-866

[25] Diana C. Landaverde-Cortes and Gustavo A. Iglesias-Silva, *Densities and Viscosities of MTBE + Nonane or Decane at p = 0.1 MPa from (273.15 to 363.15) K,* J. Chem. Eng. Data 2008, 53, 288-292

[26] D. R. Caudwell, J. P. M. Trusler, V. Vesovic, W. A. Wakeham, *The Viscosity and Density of n-Dodecane and n-Octadecane at Pressures up to 200 MPa and Temperatures up to 473 K,* International Journal of Thermophysics,September 2004, Volume 25, Issue 5, pp 1339-1352

[27] David van der Spoel, Paul J. van Maaren, and Herman J. C. Berendsen, *A systematic study of water models for molecular simulation: Derivation of water models optimized for use with a reaction field,* J. Chem. Phys. 1998, 108, 10220

[28] Susana Zeppieri, Jhosgre Rodriguez, and A. L. Lopez de Ramos, *Interfacial Tension of Alkane + Water Systems,* J. Chem. Eng. Data 2001, 46, 1086-1088

Appendix A

Force Fields

Here, we have discussed some of the commonly used force field which is supplementary to the discussion we had in "force field" topic in "Computational Methods" section.

DREIDING:

DREIDING was developed to have a generic approach to the Force Fields(FF) that deliberately obeys simple rules. This can lead to lower level of accuracy for some generalized set of molecules but it will allow reasonable predictions for novel combination of elements[13].

Bond-stretching term in DREIDING can be written as Morse function apart from having the conventional harmonic oscillator form

$$E_B = D_e[e^{(-\alpha nR - R_e)} - 1]^2 \tag{A.1}$$

Morse function is more accurate as it includes the anharmonic terms near equilibrium(R_e) and leads to the finite energy(D_e) in order for the bond to break. Here, α is the Morse scale parameter. Angle bending term is harmonic. The torsional term looks like

$$E_T = \frac{1}{2}V(1 - cos[n(\phi - \phi_0)]) \tag{A.2}$$

where ϕ is the dihedral angle, n is the periodicity(an integer), V is the barrier to the rotation and ϕ_0 is the equilibrium angle. The non-bonded terms are standard LJ and Coulombic terms.

The DREIDING force field was designed for predicting structures and dynamics of organic, biological, and main-group inorganic molecules. The validation of this FF was done by calculating properties like crystal structures of organic compounds, rotational barriers, relative conformational energies of various organic systems.

AMBER:

The AMBER95 for protein is one of the FF which has been developed along the development of MD simulation software packages[14]. As partial charges in a protein

structure are critical, these charges have been calculated using Restrained Electrostatic Potential(RESP) method while charges in OPLS-AA are derived using liquid properties as a guide. Further studies have been performed to access how good the method performed in calculating conformational energies and it turns out that it fared better than other Force Fields[15].

The model presented in Amber can be described as the "minimalist" in it's functional form where bond and angle terms are in harmonic form, VDW interaction is modeled by 6-12 potential(LJ potential) while electrostatic interactions has been modeled by Coulombic intercations and dihedral term has been defined as

$$E_T = \sum_{dihedrals} \frac{V_n}{2}[1 + cos(n\phi - \gamma)] \tag{A.3}$$

where ϕ is the dihedral angle. Non-bonded interactions are calculated between atoms which are separated by at least three bonds("1-4 interactions").

This FF has been verified by calculating conformational energies, free energies of solvation, interaction energies of proteins and nucleic acids etc.

CHARMM(Chemistry at HARvard Molecular Mechanics):

In the CHARMM force field[16] the atomic charges has been derived from ab initio quantum chemical calculations of the interactions between model compounds and water molecules. The dihedral parameter optimization process included results from MD simulations on multiple DNA and RNA structures for which experimental data is available. The optimization of non-bonded parameters was done by reproducing QM minimum interaction energies and geometries and experimental crystal data.

This approach provides a FF that properly balance out the interaction triad: solute-solute, solute-solvent and solvent-solvent non-bonded interactions. This balance is essential to obtain accurate structural and thermodynamic properties for the MD simulations in the condensed phase.

Here bond and angle terms are in harmonic form, VDW interaction is modeled by 6-12 potential(LJ potential) while electrostatic interactions has been modeled by Coulombic intercations and dihedral term has been defined as

$$E_T = \sum_{dihedrals} K_\chi(1 + cos(n\chi - \delta)) \tag{A.4}$$

where χ is the dihedral angle, n is the multiplicity and δ is the phase which represents the location of minima and maxima.

The optimization of the internal parameters was done using experimental gas-phase geometries, vibrational spectra, and torsional energy surfaces supplemented with ab initio results[17]. In addition, dipole moments, experimental heats and free energies of vaporization, solvation and sublimation, molecular volumes, and crystal pressures and structures were used in the optimization.

OPLS(Optimized Potentials for Liquid Sumlations):

Most of the bond-stretching and angle-bending parameters has been extracted from the AMBER95 or CHARMM22 FF. The torsional and non-bonded parameters has

been derived using a mix of ab initio molecular orbital calculations and Monte Carlo simulations[18].

As usual, bond and angle terms are in harmonic form, VDW interaction is modeled by 6-12 potential(LJ potential) while electrostatic interactions has been modeled by Coulombic intercations and dihedral term has been defined as

$$E_T = \sum_i \frac{V_1^i}{2}[1+cos(\phi_i+f_1)]+\frac{V_2^i}{2}[1-cos(2\phi_i+f_2)]+\frac{V_3^i}{2}[1+cos(3\phi_i+f_3)] \quad \text{(A.5)}$$

where ϕ_i is the dihedral angle, V_1, V_2 and V_3 are the coefficients in the Fourier series, and f_1, f_2 and f_3 are phase angles which are all zero for n-alkanes.

The average errors in $\triangle H_{vap}$ for hydrocarbons is 2 $\%$ for both OPLS-AA and OPLS-UA while the average errors in densities is 3 $\%$ from OPLS-AA and 2 $\%$ from OPLS-UA. The OPLS-UA models for alcohols(includes phenol) gave average errors of 1.3 $\%$ for $\triangle H_{vap}$ and 1.8 $\%$ for densities. The corresponding errors for alcohols with OPLS-AA model are 2.2 $\%$ and 1.8 $\%$.